# In-situ deuteration study of LaFeSi into superconducting LaFeSi(H,D)

Mads Fonager Hansen, Jean-Baptiste Vaney, Patricia de Rango, Mathieu Salaun, Sophie Tencé, V. Nassif, Pierre Toulemonde

# In-situ deuteration study of LaFeSi into superconducting LaFeSi(H,D)

M. F. Hansen,[1] J.-B. Vaney,[2] P. De Rango,[1] M. Salaün,[1] S. Tencé,[2] V. Nassif,[1,3] and P. Toulemonde[1]

[1]*CNRS, Université Grenoble Alpes, Institut Néel, 38042 Grenoble, France*
[2]*CNRS, Université Bordeaux, ICMCB, UPR 9048, F-33600 Pessac, France*
*3 Institut Laue-Langevin, 71 Avenue des Martyrs, 38000 Grenoble cedex 9, France*

(Dated: December 1, 2022)

In this study we investigate the topotactical deuteration of LaFeSi using *in-situ* neutron powder diffraction, yielding superconducting LaFeSi(H,D). The structural changes are linked to the thermodynamic nature of the chemical process, investigated using thermogravimetric analysis, differential thermal analysis, and mass spectroscopy. Pressure-composition-isotherm measurements further show a remarkably low equilibrium pressure. The reaction is found to be binary with the two phases LaFeSi and LaFeSiD coexisting during the reaction. The reaction enthalpy, determined using differential thermal analysis is found to be $\Delta$H = -54.5 kJ/mol. Furthermore the anisotropy of the thermal expansion is observed to change significantly as $\alpha_c/\alpha_a$ changes from 6.6 to 1.2. All the LaFeSi(H,D) obtained samples were found superconducting with $T_c \sim 10$ K, i.e. the value corresponding to stoichiometric composition. We conclude that this gas-solid process is not suitable for controlling the hydrogen x(H) content in $LaFeSiH_x$ and so to tune the related $T_c$.

## I. INTRODUCTION

Since the discovery of superconductivity in the $LaFeAsO_xF_{1-x}$ system [1], iron based superconductors (IBSC) have been rigorously researched due to the unconventional pairing mechanism and the promisingly high $T_c$s which have been realized in this family of compounds. It has been clear since the beginning that controlling the doping of these compounds is key in tuning the superconducting properties. Such control can be achieved through several different approaches, as was done in the in the LaFeAs(O/H/F) system i.e. chemical substitution [2, 3] or mechanical pressure [4–6]. It can be very challenging to control the occupancy of light elements in a heavy element based compound since no non-destructive technique is available which can accurately assign the occupancy of e.g. hydrogen in such materials without the use of large scale facilities. Therefore it is important to understand the chemistry of the reactions used in synthesis of these kind of materials, as it sets the limits for the control of the superconducting properties.

In 2018, superconductivity was discovered in LaFeSiH, below $T_c \sim 10$ K, further expanded the range of iron-based superconductors beyond the chalcogenides/pnictides which traditionally form the family of IBSCs [7]. In this system the synthesis route is quite different from that used in the arsenides where a lot of the s called 1111-type compounds were synthesised using high pressure techniques [8–10]. LaFeSiH was synthesised by topotactical insertion of hydrogen into the $La_4$ tetrahedral site of the intermetallic compound LaFeSi, yielding a ZrCuSiAs-type structure. In fact, it turns out that several compounds can be realized using this method, through the insertion of F [11] or O [12] in place of H, with $T_c$ in the 7-10 K range. This synthesis route allows the investigation of thermodynamic properties and chemical pathways using techniques commonly used in the hydrogen storage materials community.

In this study we investigate the thermodynamic properties of the topotactical deuteration process of LaFeSi by using thermogravimetric analysis coupled with differential thermal analysis and mass spectroscopy (TGA/DTA/MS). We also investigate the equilibrium pressure of the deuteration using pressure-temperature-isotherm (PCI) measurements. These properties are linked to the structural transformation by *in-situ* neutron powder diffraction (NPD).

## II. EXPERIMENTAL

### A. Synthesis of LaFeSi

Polycrystalline LaFeSi samples, of masses between 2 g and 4 g, were synthesized by arc melting in a high-purity argon atmosphere, from a stoichiometric mixture of pure elements with a La excess of 2 % (Fe Alfa Aesar 99.95 %, Si Alfa Aesar 99.9995 %, La 99.9 % Alfa Aesar). The boules were turned upside down and remelted several times to ensure chemical homogeneity. Prior to this step, pure La was pre-melted in an induction furnace for several minutes to evaporate volatile oxides and impurities. These samples were subsequently ground and cold pressed into pellets then annealed in evacuated quartz tubes for 10 days at 950 °C.

### B. Thermo graviometric analysis, differental thermal analysis, and mass spectrometry

For the TGA/DTA/MS (Thermogravimetry / Differential thermal analysis / Mass spectrometry) measurements, a 70 $\mu$L alumina crucible was filled with 70.6 mg of LaFeSi (estimated 93.5 (wt) % purity based on XRD, see S.I.) and placed in a symmetrical TGA/DTA system (Setaram TAG 16) coupled with a mass spectrometer (Hiden QGA). The sample and compensation chambers were in the same and constant gas flow of $Ar/H_2$ to avoid any

mass drift due the Archimed force of the gas flow on the sample. The gas flow consisted of 10 % $H_2$ and 90 % Ar from a bottle (Air Liquide HYD-105). The temperature was increased using a ramp of 1 °C/min to a maximum temperature of 500 °C. During the experiment, the relative abundance of a large range (m/z = 1-50) in the exhausted gas were followed by the MS system. Here m/z = 2 corresponds to dihydrogen, m/z = 40 and m/z = 20 correspond to Argon. After the experiment, the measurement was repeated using the hydrogenated sample and this second measurement was used a background subtraction. The DTA sensitivity in the temperature range was calibrated using the melting of Zn (99,999 %) at 419.5 °C.

### C. Pressure-Composition-Isotherm

To measure the PCI curves, a sample of LaFeSi was placed in a HIDEN PCI system. Three different isotherms were measured (T = 200°C, 300°C, 450°C), recording the pressure evolution, as gas is systematically injected into the sample container. Between each isotherm the sample was desorbed under a secondary vacuum for 24h at 500°C to recover LaFeSi. A typical XRD pattern before and after a PCI run is shown in S.I.

### D. Neutron powder diffraction

NPD was performed at the D1B instrument of the ILL [13]. 1.6516 g of LaFeSi (95 %) powder was placed in a vanadium tube connected to a cryo-furnace and a HIDEN PCI setup. The sample was heated to 180 °C in 2 hours and 20 minutes, while kept under vacuum and the temperature was stabilized. During heating, neutron diffraction patterns were recorded with a counting time of 1 min, the first 48 minutes where-after the counting time was increased to 2 minutes. Deuterium was then injected into the sample chamber with a maximum pressure in the ante-chamber of 1 bar, leading to a maximum pressure change in the sample chamber of 0.5 bar since the sample chamber and ante-chamber are similar in size. NPD patterns were continuously collected with a counting time of 3 minutes pr pattern with a wavelength of 1.28 Å during the temperature plateau. Gas injections were performed during the collection as the sample chamber pressure decreased, to keep the reaction running. The temperature plateau at 180 °C was 12.5 hours long. The first NPD acquisition and initiation of the first gas injection cycle were synchronized such that the gas pressure in the chamber and the recorded NPD patterns can be correlated in time. The sample was then cooled down in 72 minutes, while neutron diffraction patterns were collected with a 3 minute counting time. The structural parameters were extracted using the Rietveld method, in the Fullprof software [14].

### E. Resistivity

Resistivity measurements were carried out as four point measurements on powders compressed to a pellet using a cold press. A Keithley 6220 Precision current source was used to provide the current for our measurements. The voltage was measured using a Keithley 2182A nanovoltmeter. The samples were placed in a "Precision Cryogenic Systems, Inc." He-cryostat for low temperature measurements, down to T = 2.5 K.

## III. RESULTS AND DISCUSSION

### A. Pressure composition isotherm

Towards understanding the thermodynamics of the LaFeSi hydrogenation process, three hydrogen absorption isotherms were measured at 200 °C, 300 °C and 450 °C, shown in figure 1. Looking at the isotherms we mark the very low pressure range of the pressure plateaus, showing that the equilibrium pressure of this reaction is in the mbar range. An ideal and completely flat plateau pressure is not reached and the exact determination of the equilibrium pressure thus becomes difficult. Furthermore the error on the data points is very large compared to the change in equilibrium pressure in the measured temperature range.

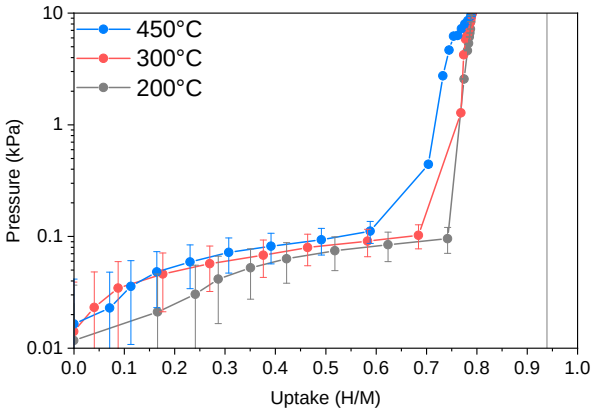


FIG. 1. The three different pressure composition isotherms measured using a HIDEN PCI setup for the LaFeSi hydrogenation process. The errors are based on the hardware specifications as 0.25 %.

Extracting thermodynamic parameters such as the reaction enthalpy or the entropy change with the ususal Van't Hoff analysis is difficult based on this PCI measurement, given the very low equilibrium pressure range. Considering trends among hydrogen storage materials, the having a low equilibrium pressure means that the metal-hydride has a high stability and we should thus expect to find a rather high reaction enthalpy [15].

### B. Thermogravimetric analysis, differental thermal analysis and mass spectrometry

Given the low equilibrium pressure, the thermodynamics can be probed by other means, not relying on measurements of pressure. One such method is the use of DTA. In figure 2 we show an in-situ measurement of the hydrogenation process of LaFeSi using TGA/DTA/MS. First, at a temperature of $T_{onset}$ = 272 °C we see a notable increase in the TG signal. This increase becomes linear at temperatures above 350 °C. The expected mass increase upon hydrogenation of LaFeSi, $\Delta m = 0.318$ mg, is consistent with the observed mass increase, if one considered the linear mass increase to be extrinsic. The nature of such linear increase in the TG signal, however, is not clear. Then, around the same temperature we observe a drop in the relative abundance of hydrogen, calculated here from the partial pressure, considering all channels between m/z = 1 and m/z = 50 from the mass spectrometer and having the total pressure normalized to 1 (see all channels in figure 3 in S.I.) The drop in the MS signal is consistent with the uptake of hydrogen into the intermetallic, LaFeSi, and further, the re-stabilization of the partial pressure after this local minimum, further supports an extrinsic nature of the linear mass increase.

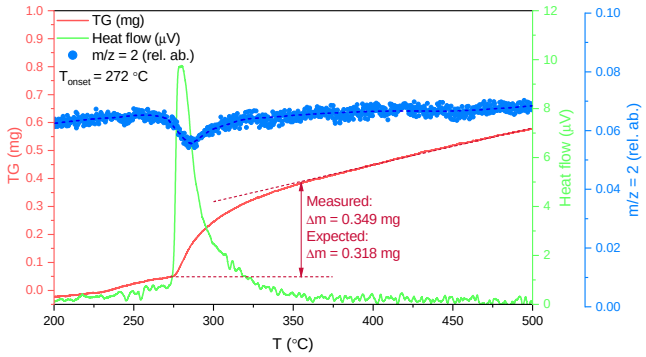


FIG. 2. The TG signal, heat flow and the relative abundance of $H_2$ as measured by mass spectroscopy during the hydrogenation of LaFeSi

The DTA signal shows an exothermic peak around the same temperature where the mass increase and the decrease in the relative abundance of hydrogen. By integrating the signal gives a value of the phenomenon of 133.38 $\mu$V·s/mg which correspond to an enthalpy change of $\Delta H$ = -54.5 kJ/mol, associated with the uptake of hydrogen in LaFeSi. The reaction enthalpy is thus rather high for this reaction, indicating a high stability of the hydride. This is also in line with the observation of a low equilibrium pressure. Comparing this to the enthalpy of formation of e.g. $MgH_2$, $\Delta H$ = -74 kJ/mol, we see that the value is in a similar range [16].

### C. In-situ deuteration of LaFeSi using neutron powder diffraction

Then, to link this reaction to the crystallographic structure we performed in-situ deuteration of LaFeSi using NPD. In figure 3.a we show the diffraction patterns recorded throughout the entire experiment. The experiment is divided into three different sections: heating, deuteration, and cooling. First, we will discuss the deuteration process. From the patterns, a strong decrease in the contributions from the LaFeSi phase is observed simultaneously with the emergence of a new phase, which can be indexed as tetragonal LaFeSiD. This transition happens around 1 hour after the first injection. The delay in the reaction is due to the incubation time of the reaction, which is common place for hydrogenation reactions. In figure 3.b, we show a section of the diffraction pattern at three different times, where $t_0$ = 0h is set to be the start of the deuteration process, $t_1$ = 1h15, and $t_2$ = 12h30, as indicated in 3.a. The expected positions of reflections corresponding to LaFeSi and LaFeSiD are shown in blue and red, respectively. From the data, we can see the lack of an intensity continuum between e.g. the (112) reflections of the two phases. This indicates that the formation of LaFeSiD from LaFeSi happens as a binary process, in contrast to a continuous deuteration [17–19]. The peak shape and unit cell parameters of LaFeSi, LaFeSiD and $LaFe_2Si_2$ were refined using the patterns collected before and after the deuteration. These parameters were used in a sequential refinement which varied only the scale factor. The atomic positions were assumed the same as reported by Welter et al.[20] and Bernardini et al.[7] for LaFeSi and LaFeSiH respectively.

From the refinements, the volume fraction of the three phases were calculated as a function of time during the deuteration process. In figure 3.c we show the evolution of the phase distribution, plotted together with the deuterium uptake calculated from the measurements of the pressure above the sample. There is a very good agreement between the weight fraction of LaFeSiD obtained from diffraction and the calculated value from the pressure change.

Turning now to the two other parts of the experiment, the heating and the cooling. The unit cell parameters were followed during the heating and cooling of the sample, i.e. before and after the deuteration process. From the refined models we obtain the temperature dependence of the unit cell parameters, shown in figure 4. In the 20 - 180 °C range, their behaviors are linear in temperature, without any anomaly.

The Deuteration of LaFeSi results in a significant expansion of the $c$-axis, $\sim$ 1 %, as shown in figure 4.a. The $a$-axis, however, shows a slight contraction upon Deuteration,$\sim$ 1 %, as seen in figure 4.b. This behavior was also reported by Bernardini et al. [7]. Despite the contraction in the $a$-axis the volume of the unit-cell, shown in figure 4.c is expanded by approximately 10%,

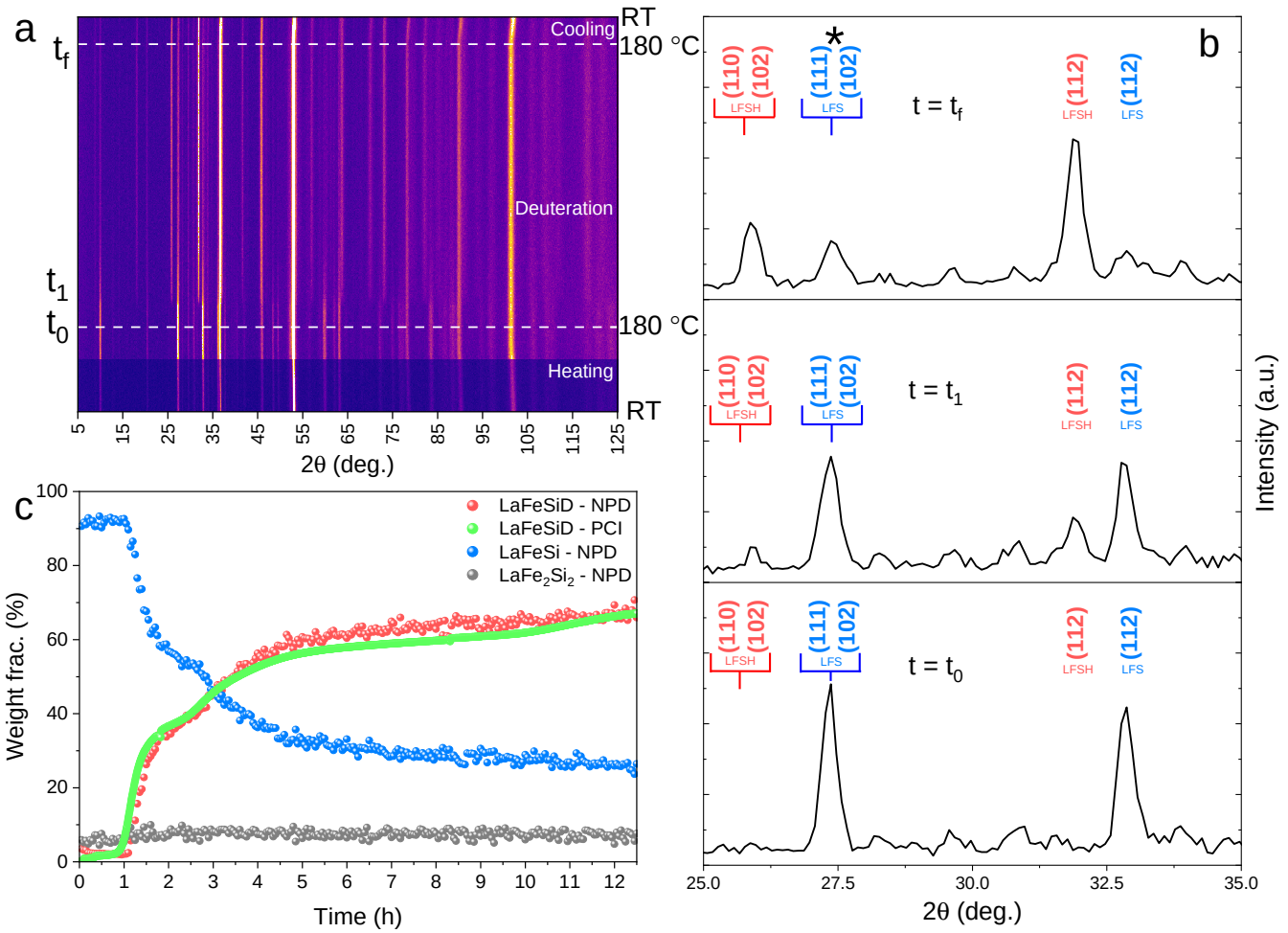


FIG. 3. Data and results of in-situ neutron diffraction study (with $\lambda = 1.28$ Å) of the deuteration process of LaFeSi. **a:** The neutron diffraction patterns recorded during heating, deuteration, and cooling. **b:** The neutron diffraction patterns at three different times during the deuteration process with $t = t_0 = 0$ corresponding to the time of the first gas injection. The star indicates that the LaFeSiD phase is also expected to produce intensity at this angle, corresponding to the (111) and (005) reflections. **c:** The weight fraction of the main phases, LaFeSi and LaFeSiD during the deuteration process as well as the secondary phase $LaFe_2Si_2$, obtained by the Rietveld method.

though this expansion is obviously highly anisotropic.

TABLE I. The thermal expansion coefficients for the a-axis, c-axis and volume of LaFeSi and LaFeSiD, as calculated from the slope of the curves shown in figure 4 and initial 300 K values, obtained from neutron diffraction.

| $10^{-5}$ K$^{-1}$ | LaFeSi | LaFeSiD |
|---|---|---|
| $\alpha_{a,300K}$ | 0.4(1) | 2.5(5) |
| $\alpha_{c,300K}$ | 2.9(3) | 3.0(1) |
| $\alpha_{V,300K}$ | 2.6(2) | 3.9(2) |

From the slope of the unit cell parameters we obtain the thermal expansion coefficients at 300 K for $a$, $c$ and the volume, these are given in table I. Interestingly the largest change in thermal expansion coefficient is for the $a$-axis. This also means that the anisotropy of the thermal expansion which can be described as $\alpha_c/\alpha_a$ changes from 6.6 to 1.2 making it significantly more isotropic in LaFeSiD as opposed to LaFeSi, despite LaFeSiD having a more anisotropic unit cell.

### D. Superconductivity of the deuterated recovered samples

In figure 5 we show the resistance as a function of temperature measured for a cold pressed pellet of LaFeSiD, as obtained after the NPD experiment described above. We observe a drop in the resistance at 10 K which moves to lower temperature as the external magnetic field is increased, consistent with a superconducting transition. The transition is in the same temperature range as previously reported for LaFeSiH [7]. The transition is not complete and constitutes around 36% of the normal state resistance. We attribute this to resistive grain boundaries, an effect which has also been observed in e.g. $LaFeSiO_{1-\delta}$

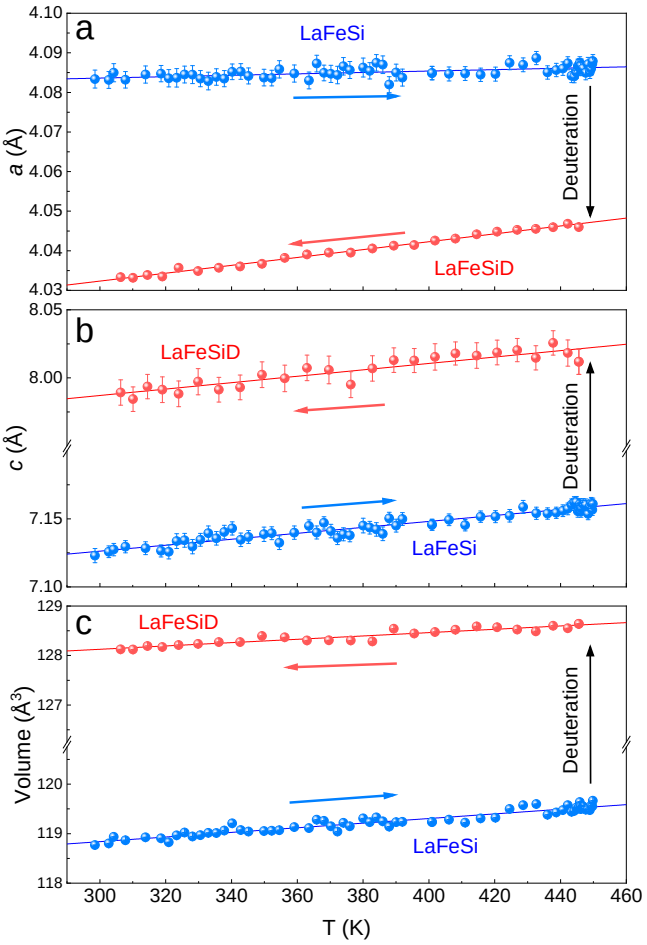


FIG. 4. The evolution of the refined unit cell parameters of LaFeSi (in blue) and LaFeSiD (in red) during temperature cycling and gas injection. **a:** The $c$-axis, expanding upon insertion of Deuterium. **b:** The $a$-axis contracting slightly upon insertion of Deuterium.

[12]. Measurements of the sample which was hydrogenated as a part of the TGA/DTA/MS experiment show similar behaviour (see fig. 4 in S.I.).

## IV. CONCLUSIONS

Considering the results of the NPD experiment, the deuteration of LaFeSi can be described with the binary reaction scheme, as shown in equation 1.

$$2LaFeSi_{(s)} + H_{2(g)} \rightleftharpoons 2LaFeSiH_{(s)} \qquad (1)$$

The phases LaFeSiD and LaFeSi coexist during the deuteration and no partially hydrogenated $LaFeSiH_x$ with $0 \leq x(H) \leq 1$ (or intermediate phase) is formed. This is clearly evidenced by the lack of a continuum between the Bragg peaks belonging to LaFeSi and LaFeSiD.

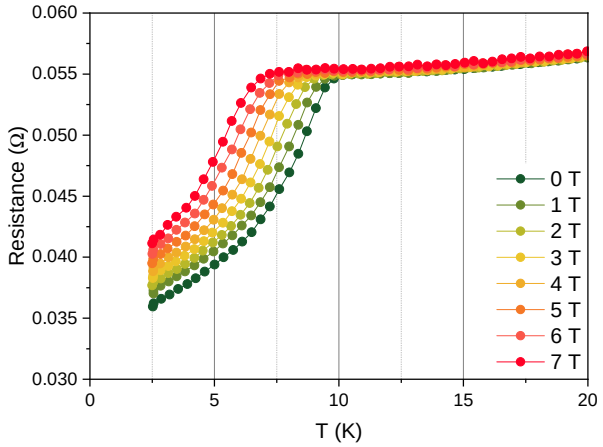


FIG. 5. Resistance of a poly-crystalline as a function of temperature as a function of temperature, measured after deuteration at the ILL.

The deuteration of LaFeSi is an exothermic, enthalpy driven, reaction with a reaction enthalpy of $\Delta H$ = -54.5 kJ/mol. Remarkably, the equilibrium pressure is very low, on the order of 1 mbar in the investigated temperature regime. Furthermore we have determined the thermal expansion coefficients of LaFeSi and LaFeSiD, in the 20 - 180 °C range, to be $\alpha_{V,300K} = 2.6(2)\cdot10^{-5}$ $K^{-1}$ and $\alpha_{V,300K} = 3.9(2)\cdot10^{-5}$ $K^{-1}$ respectively. The obtained LaFeSi(H,D) compounds were checked to be superconducting with $T_c \sim$ 8-10 K as reported previously for stoichiometric LaFeSiH [7]. We conclude that this gas-solid pathway is not suited for obtaining homogeneous, partially hydrogenation $LaFeSiH_x$, with tunable $T_c$.

## V. ACKNOWLEDGEMENT

We would like to acknowledge Paul Chometon for his help in performing TGA/DTA/MS measurements. Further, we want to acknowledge the Frederic Gay and Florent Blondelle for assistance in resistivity measurements.

[1] Y. Kamihara, T. Watanabe, M. Hirano, and H. Hosono, Journal of the American Chemical Society **130**, 3296 (2008).

[2] J. Zhao, Q. Huang, C. de la Cruz, S. Li, J. W. Lynn, Y. Chen, M. A. Green, G. F. Chen, G. Li, Z. Li, J. L. Luo, N. L. Wang, and P. Dai, Nature Materials **7**, 953 (2008).

[3] Q. Huang, J. Zhao, J. W. Lynn, G. F. Chen, J. L. Luo, N. L. Wang, and P. Dai, Phys. Rev. B **78**, 054529 (2008).

[4] N. Takeshita, A. Iyo, H. Eisaki, H. Kito, and T. Ito, Journal of the Physical Society of Japan **77**, 075003 (2008), https://doi.org/10.1143/JPSJ.77.075003.

[5] N. Kawaguchi, N. Fujiwara, S. Iimura, S. Matsuishi, and H. Hosono, Phys. Rev. B **94**, 161104 (2016).

[6] K. Kobayashi, J.-i. Yamaura, S. Iimura, S. Maki, H. Sagayama, R. Kumai, Y. Murakami, H. Takahashi, S. Matsuishi, and H. Hosono, Scientific Reports **6**, 39646 (2016).

[7] F. Bernardini, G. Garbarino, A. Sulpice, M. Núñez Regueiro, E. Gaudin, B. Chevalier, M.-A. Méasson, A. Cano, and S. Tencé, Phys. Rev. B **97**, 100504 (2018).

[8] S. Iimura and H. Hosono, Journal of the Physical Society of Japan **89**, 051006 (2020), https://doi.org/10.7566/JPSJ.89.051006.

[9] K. Miyazawa, K. Kihou, P. M. Shirage, C.-H. Lee, H. Kito, H. Eisaki, and A. Iyo, Journal of the Physical Society of Japan **78**, 034712 (2009), https://doi.org/10.1143/JPSJ.78.034712.

[10] J.-W. G. Bos, G. B. S. Penny, J. A. Rodgers, D. A. Sokolov, A. D. Huxley, and J. P. Attfield, Chem. Commun. , 3634 (2008).

[11] J.-B. Vaney, B. Vignolle, A. Demourgues, E. Gaudin, E. Durand, C. Labrugère, F. Bernardini, A. Cano, and S. Tencé, Nature Communications **13**, 1462 (2022).

[12] M. F. Hansen, J.-B. Vaney, C. Lepoittevin, F. Bernardini, E. Gaudin, V. Nassif, M.-A. Méasson, A. Sulpice, H. Mayaffre, M.-H. Julien, S. Tencé, A. Cano, and P. Toulemonde, npj Quantum Materials **7**, 86 (2022).

[13] M. F. Hansen, I. P. Orench, S. Tence, P. Toulemonde, J. B. Vaney, and V. Nassif, Institut Laue-Langevin (ILL) - (2021), http://doi.ill.fr/10.5291/ILL-DATA.5-24-657.

[14] J. Rodriguez-Carvajal, in *satellite meeting on powder diffraction of the XV congress of the IUCr*, Vol. 127 (Toulouse, France, 1990).

[15] F. Marques, M. Balcerzak, F. Winkelmann, G. Zepon, and M. Felderhoff, Energy Environ. Sci. **14**, 5191 (2021).

[16] M. Paskevicius, D. A. Sheppard, and C. E. Buckley, Journal of the American Chemical Society **132**, 5077 (2010), pMID: 20307102, https://doi.org/10.1021/ja908398u.

[17] J. W. Makepeace, M. O. Jones, S. K. Callear, P. P. Edwards, and W. I. F. David, Phys. Chem. Chem. Phys. **16**, 4061 (2014).

[18] P. de Rango, A. Chaise, J. Charbonnier, D. Fruchart, M. Jehan, P. Marty, S. Miraglia, S. Rivoirard, and N. Skryabina, Journal of Alloys and Compounds **446-447**, 52 (2007), proceedings of the International Symposium on Metal-Hydrogen Systems, Fundamentals and Applications (MH2006).

[19] I. Popa, S. Rivoirard, P. de Rango, and D. Fruchart, Journal of Alloys and Compounds **428**, 44 (2007).

[20] R. Welter, G. Venturini, and B. Malaman, Journal of Alloys and Compounds **189**, 49 (1992).